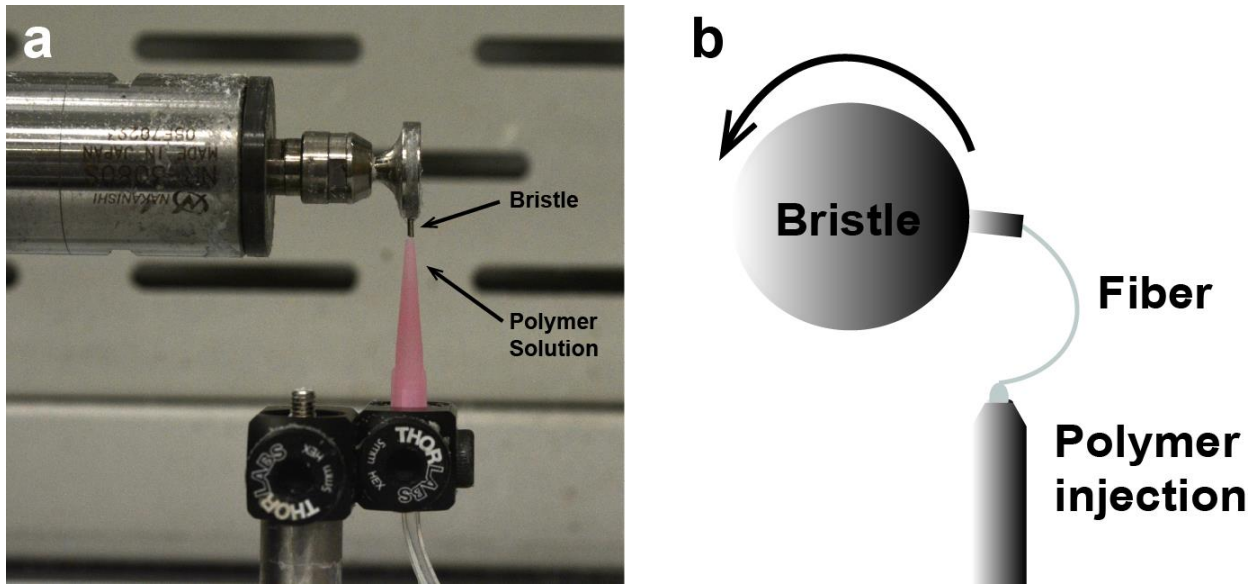


1 **Supporting Information**

2



3

4 **Figure S1.** Image illustrating the pull spinning system used for nanofiber fabrication.

5

6

7

8

9

10

11

12

13

14

15

16

17

18

19

20

21

22

23

24

25

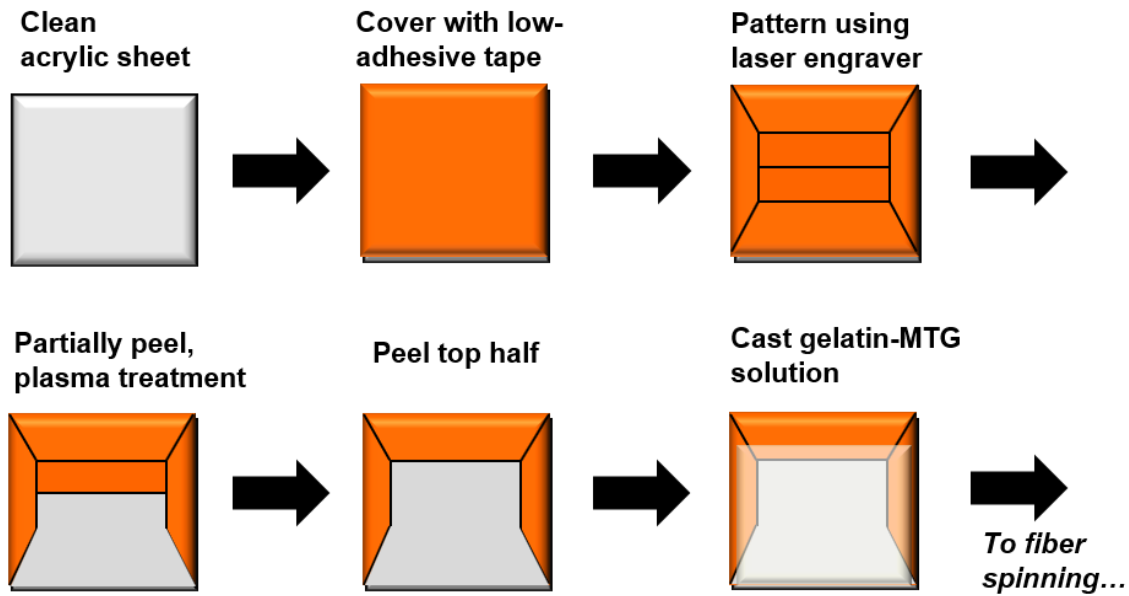
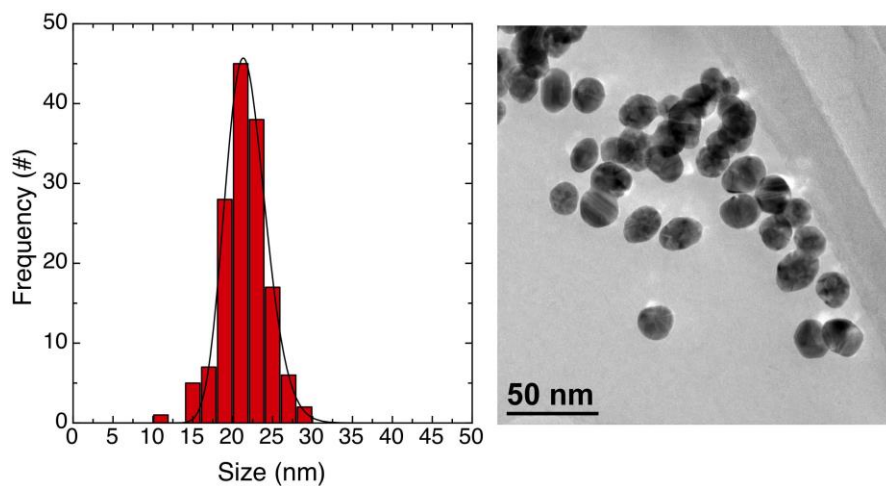
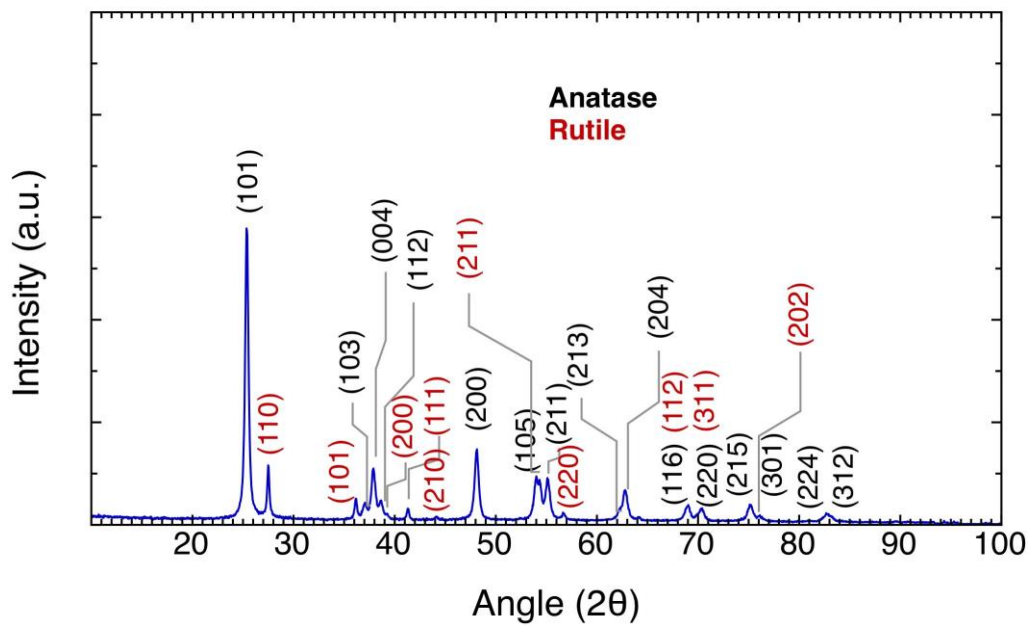


Figure S2. Schematic diagram showing the preparation of gelatin MPS substrates before spinning the fibers.

1
2
3
4
5
6
7
8
9
10
11
12
13
14
15
16
17
18
19
20
21
22



1
2 **Figure S3.** TEM Feret size distribution for the Ag nanoparticles.
3
4
5
6
7
8
9
10
11
12
13
14
15
16
17
18
19
20
21
22
23
24
25
26
27
28
29
30
31



1
2
3
4
5
6
7
8
9
10
11
12
13
14
15
16
17
18
19

Figure S4. XRD Pattern for the TiO₂ Degussa P25.

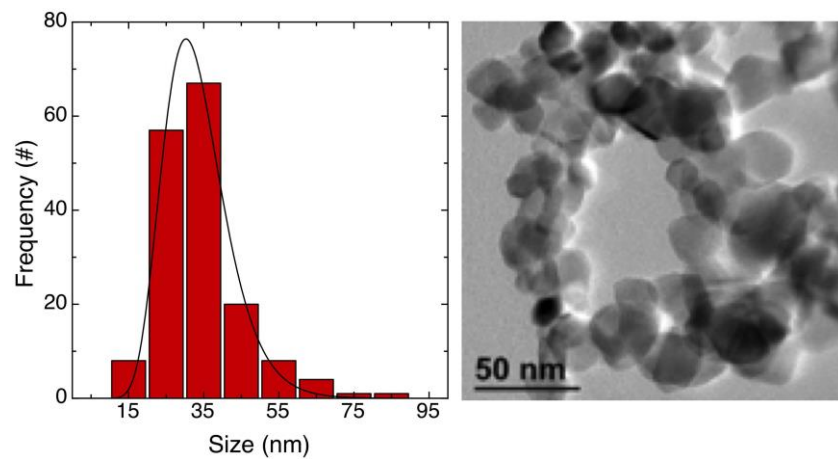
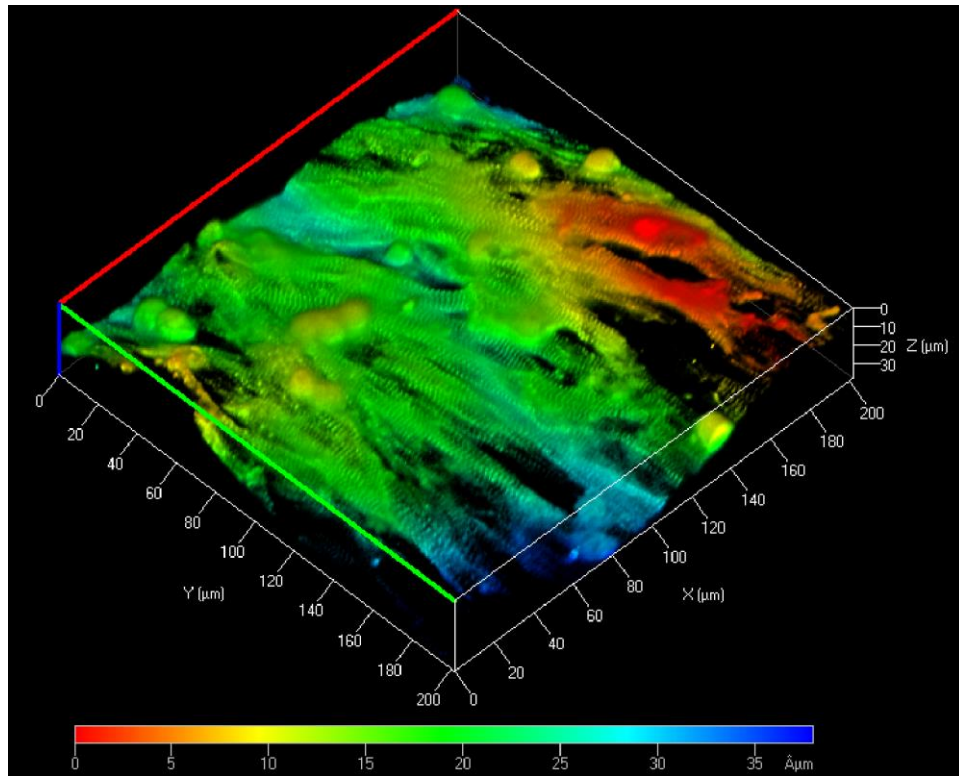


Figure S5. TEM Feret size distribution for the TiO₂ Degussa P25.

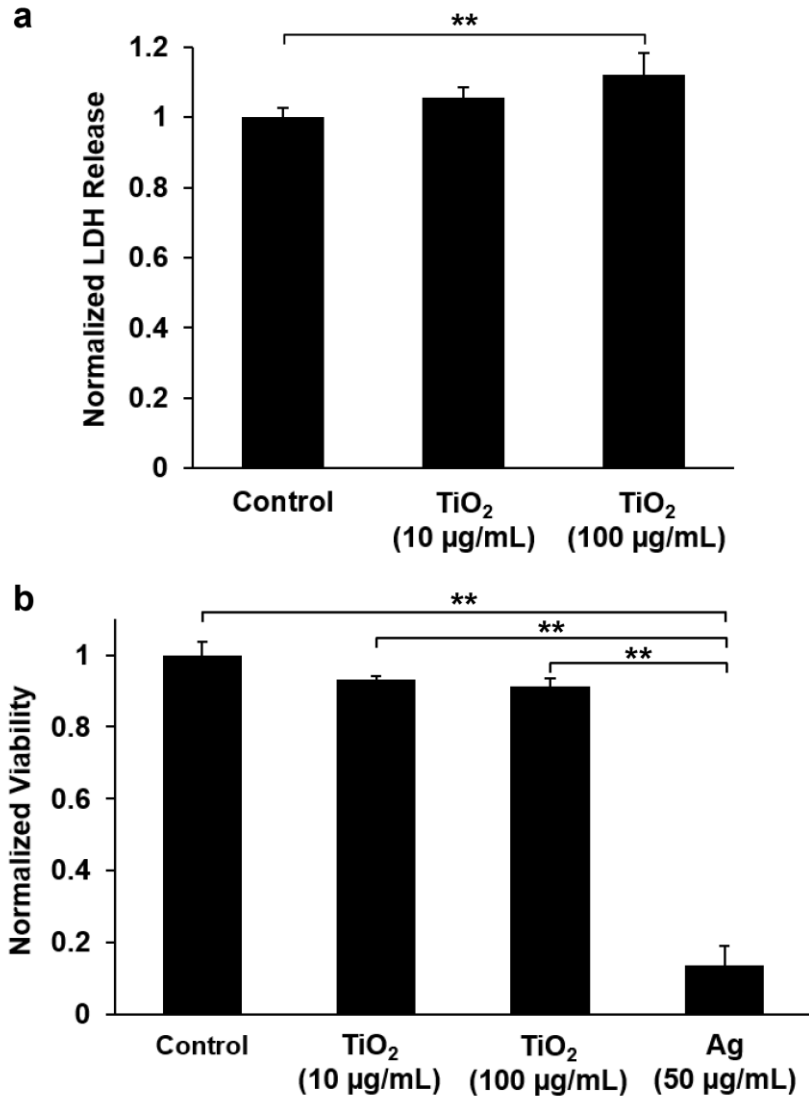
1
2
3
4
5
6
7
8
9
10
11
12
13
14
15
16
17
18
19
20
21
22
23
24
25
26
27
28
29
30
31
32

1



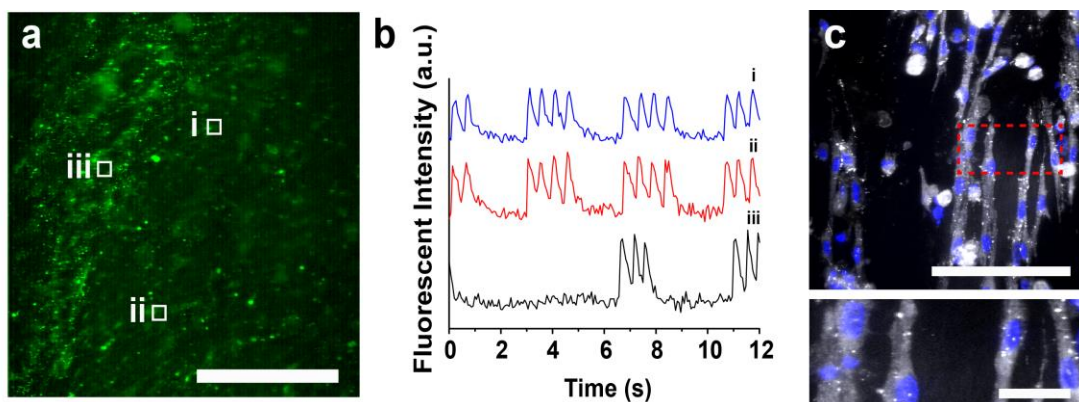
2

3 **Figure S6.** Representative 3D reconstruction image of z-stacked confocal images of NRVMs
4 grown on PCL/PDA nanofiber scaffold with a color depth.



1
2 **Figure S7.** Cytotoxicity tests for cardiomyocytes cultured on fiber MTFs. a) Comparison of
3 lactate dehydrogenase (LDH) release of cardiomyocyte MTFs, pre- and post-exposure to TiO₂ at
4 10 and 100 µg/mL. b) Comparison of cell viability based on MTT assay for cardiomyocytes
5 unexposed and exposed to 50 µg/mL Ag nanoparticles. Bars represent standard error, *n*=8 per
6 condition for LDH assay, *n*=16 for MTT assay. For statistical comparison, ***p*<0.05.

7
8
9
10
11
12
13
14
15



1
2 **Figure S8.** Effect of silver nanoparticle exposure. a–b) Confocal images of calcium dye
3 fluorescent (green) with calcium transient at the specific points (white boxes) for Ag (50 μ g/ml)
4 exposure. Scale is 500 μ m. c) Confocal image of cardiomyocytes on nanofiber, stained for nuclei
5 (blue) and α -actinin (grey). Scales are 100 μ m (for the top panels) and 20 μ m (for the bottom
6 panels). The bottom panels are the zoom-in images from the red dots of the top panels.

7
8
9
10
11
12
13
14
15
16
17
18
19
20
21
22
23
24
25
26

1 **Table S1.** Morphological and structural properties of ENMs

ENM	Primary Particle Size			Crystal Structure		
	SSA (m ² /g)	d _{BET} (nm)	d _{TEM} (nm)	d _{XRD} (nm)	Crystal System	Crystallinity (%)
TiO ₂ P25	46.45 ± 2.32	29.76 ± 1.49	28.82 ± 11.07	Anatase: 21.3 Rutile: 30.40	Anatase 81.4% Rutile 16.2%	81.4
Ag – citrate capped	N/A	N/A	21.58 ± 2.83	N/A	N/A	N/A

2 ENM, engineered nanomaterial; SSA by nitrogen adsorption/Brunauer-Emmett-Teller (BET)
 3 method; d_{BET}, d_{TEM} and d_{XRD}, particle
 4
 5
 6
 7
 8
 9
 10
 11
 12
 13
 14
 15
 16
 17
 18
 19
 20
 21
 22
 23
 24
 25
 26
 27
 28
 29
 30
 31
 32
 33
 34
 35

1 **Table S2.** Physical properties of ENMs

ENM	Shape Factors			Porosity		ρ_{raw} (g/cc)
	Aspect ratio	Circularity	Roundness	TPV (cc/g)	APS [§] (nm)	
TiO ₂ P25	1.276 ± 0.162	0.926 ± 0.034	0.795 ± 0.094	0.119	5.14	4.38±0.01
Ag – citrate capped	1.175 ± 0.111	0.999 ± 0.025	0.858 ± 0.078	N/A	N/A	N/A

2 ENM, engineered nanomaterial; TPV and APS, total pore volume and average pore size,
 3 respectively determined by nitrogen adsorption/Brunauer-Emmett-Teller (BET) method; ρ_{raw} , the
 4 raw density of ENMs determined by nitrogen volume displacement (pycnometry); [§]TEM did not
 5 confirm the presence of pores but interparticle spacing instead.
 6

7
8
9
10
11
12
13
14
15
16
17
18
19
20
21

1 **Table S3.** Chemical and biological properties of ENMs

ENM	Chemical Elemental Composition				Recombinant Factor C (EU/mg) [‡]	Sterility (bacterial growth observed) [†]
	Trace Metal Analysis (%)	Carbon Content (%) [*]	Stoichiometry XPS	Stoichiometry ICP-MS		
TiO ₂ P25	99.98±4.86 Ti	0.22±0.13	TiO _{1.93}	TiO _{1.86}	< LOD	No growth
Ag – citrate capped	99.69±0.60 Ag	0.17±0.21	N/A	N/A	4.870	No growth

2 ENM, engineered nanomaterial; LOD, limit of detection; ^{*}Elemental plus organic carbon content
 3 (w/w); [‡]Suspension tested at 10 µg/ml, endotoxins in PBS is 76 EU/ml; [†]suspension tested at
 4 50µg/ml;

5
6
7
8
9
10
11
12
13
14
15
16
17
18
19
20
21
22
23
24
25
26
27
28
29
30
31
32
33
34
35

1 **Table S4.** Percentage of cantilevers beating during the time point of MPS optical recording.

Condition	% Cantilevers Beating
Control (0 $\mu\text{g/mL}$)	95.0%
TiO ₂ (10 $\mu\text{g/mL}$)	91.7%
TiO ₂ (100 $\mu\text{g/mL}$)	55.6%
Ag (50 $\mu\text{g/mL}$)	28.6%

2
3
4
5
6
7
8
9
10
11
12
13
14
15
16
17
18
19
20
21
22
23
24
25
26
27
28

1 **Supplementary Movies**

2

3 **Movie 1.** NRVM contraction on PCL/PDA nanofiber scaffolds. Scale is 100 μm .

4

5 **Movie 2.** NRVM contraction on fiber-coated gelatin MPS. Scale is 2 mm.

6

7 **Movie 3.** NRVM contraction on fiber-coated cardiac microphysiological device with embedded
8 contractility sensors.

9

10 **Movie 4.** Time-series images of a calcium-sensitive dye from cardiomyocytes grown on the
11 fiber-coated MTF sample without nanoparticle exposure.

12

13 **Movie 5.** Time-series images of a calcium-sensitive dye from cardiomyocytes grown on the
14 fiber-coated MTF sample with a low-dose TiO_2 (10 $\mu\text{g}/\text{ml}$) nanoparticle exposure.

15

16 **Movie 6.** Time-series images of a calcium-sensitive dye from cardiomyocytes grown on the
17 fiber-coated MTF sample with a high-dose TiO_2 (100 $\mu\text{g}/\text{ml}$) nanoparticle exposure.

18

19